Supplemental Figure Legend

Supplemental Figure 1. Flow assisted cell sorting (FACS) of plastic adherent bone marrow-derived human mesenchymal stem cells (hMSC) demonstrated a population highly enriched (>99%) for CD90, CD105, CD133 while devoid of (>99%) CD 34 and CD45.

Supplemental Figure 2. TGFβ superfamily members induce cytosolic Nkx2.5 in human mesenchymal stem cells (hMSC). A, Immunostaining of hMSC treated for 5 days with TGFβ (lower left), Activin-A (upper right), and BMP (lower right) demonstrated increased Nkx2.5 expression *versus* naïve controls (upper left). B, The inductive effect by TGFβ superfamily members was verified through quantitative PCR of Nkx2.5 mRNA levels normalized to Tubulin.

Supplemental Figure 3. Retinoic Acid enhancement of TGFβ effect in embryonic stem cells was recapitulated in hMSC. A, Touch-up PCR approach highlighted Nkx2.5 expression enhancement in retinoic acid treated *versus* untreated embryonic stem cells in the presence of TGFβ. B, This effect was reproduced in hMSC for Nkx2.5 and MEF2C as demonstrated on quantitative PCR normalized to tubulin.

Supplemental Figure 4. Recombinant factors needed to be applied in cocktail form to achieve nuclear translocation. Nuclear translocation of Nkx2.5, MEF2C and Gata-4 quantified following individual or combined addition of TGFβ, BMP-4, Activin-A, IGF-1, FGF-2, IL-6, α-Thrombin and retinoic acid (n=6 patients, excluding patients 3 and 9).

Supplemental Figure 5. IGF-1 and FGF-2 treatment is associated with AKT phosphorilation. A, IGF-1 or FGF-2 treatment of embryonic stem cells resulted in

phosphorylation and nuclear translocation of AKT. B, IGF-1 and FGF-2 induced AKT phosphorylation is preserved in hMSC.

Supplemental Figure 6. Cocktail induced nuclear translocation of cardiac transcription factors was dependent on IGF-1 and FGF. A, Translocation of MEF2C into the nucleus following stimulation with the complete cardiogenic cocktail was lost with removal of IGF-1 and FGF-2, B. C, AKT dependence was demonstrated with loss of nuclear translocation following addition of the AKT-P inhibitor SR13668.

Supplemental Figure 7. Guidance of patient-derived hMSC results in cardiopoietic maturation. A, Cardiopoietic guidance of non-reparative patient (Pt.) hMSC resulted in nuclear MEF2C expression indicative of cardiogenic commitment. B, hMSC derived cardiomyocytes at day 10, 15 and 20 after decrease in platelet lysate concentration (Troponin-I, top; α-actinin, bottom; and rare smooth myocyte, right) demonstrated an increase in the number of mature mitochondria versus naïve hMSC, C.

Supplemental Figure 8. Cardiopoietic hMSC demonstrate capacity for cardiac differentiation and engraftment. A, Gross evaluation of hearts 20 months after therapy reveals a limited scar within the anterior all distal to the LAD ligation. B, Low magnification (10X) immunohistological evaluation reveals a larger scar area in naïve treated *versus* cardiopoietic treated (CP-hMSC) hearts with evidence of engrafted human cells within the healed scar as demonstrated by human troponin stained myocytes co-expressing ventricular myosin light chain (MLC2v). C, High magnification (63X) evaluation demonstrates cardiomyocytes expressing human troponin co-localized with α-actinin embedded within the anterior wall of the murine heart in CP-hMSC treated hearts.

Supplemental Figure 9. Cardiopoietic hMSC demonstrate *de novo* cardiogenesis and induce expression of endogenous stem cells, with rare evidence of fusion noted. A, Rarely, human nuclei, were noted to be fused to murine nuclei on species specific genomic probing (left) as quantified by confocal histogram evaluation (right). B, Quantification of Sca-1 staining cells was found to be significantly upregulated in cariopoietic hMSC treated hearts, when compared to naïve. C, human lamin (green) and Sca-1 (yellow) staining reveals high abundance of non-human, murine Sca-1 cells in cardiopoietic hMSC treated hearts.

Supplemental Figure 10. Cardiopoietic (CP) hMSC safety is determined by pathological examination and electrocardiography. A, Infarcted hearts treated with patient derived hMSC demonstrated heart muscle repair with no evidence of aberrant growth or tumor formation. Examples of hMSC derived from four distinct patients (Pt) and transplanted into four infarcted mouse hearts. B, Cardiopoietic hMSC treated mice revealed no evidence of ventricular ectopy on Holter-type continuous ECG evaluation. C, Histological evaluation of murine brain, lung, kidney, spleen and liver revealed no evidence of abnormal cellular growth or tumorigenesis 6 months after cell delivery.

Supplemental Movies. (Microscopy) Calcium transients were appreciated in hMSC derived cardiomyocytes under electrical current stimulation. (Echocardiography) Efficacy of cardiopoietic (CP) hMSC is demonstrated by echocardiography at 1-year follow-up. Short and Long axis imaging of naïve stem cell treated hearts revealed a fibrotic and hypokinetic anterior wall most evident on apical M-Mode evaluation (Pt 11 Naïve Movies). In contrast, CP hMSC treated hearts revealed a robust contractile profile throughout the anterior wall reflecting a sustained benefit from guided stem cell therapy (Pt 11 CP Movies).

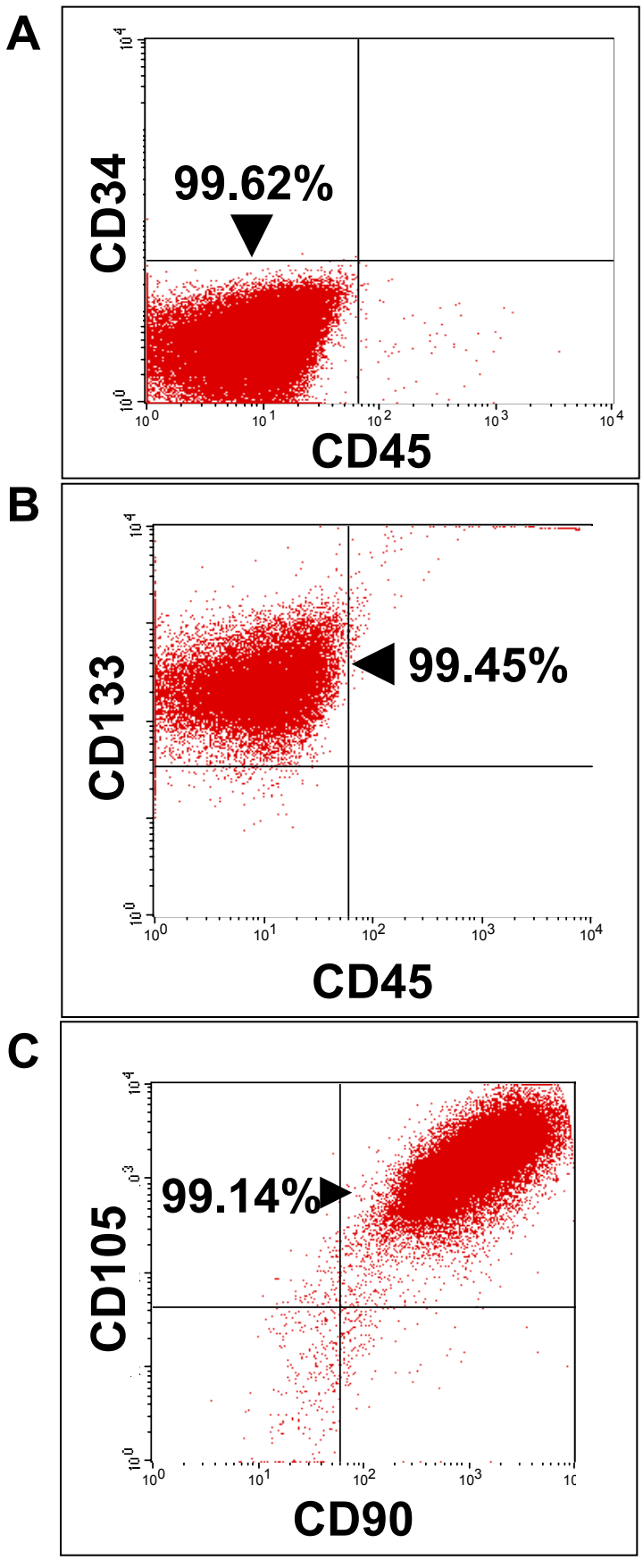

Supplemental Figure 1

A

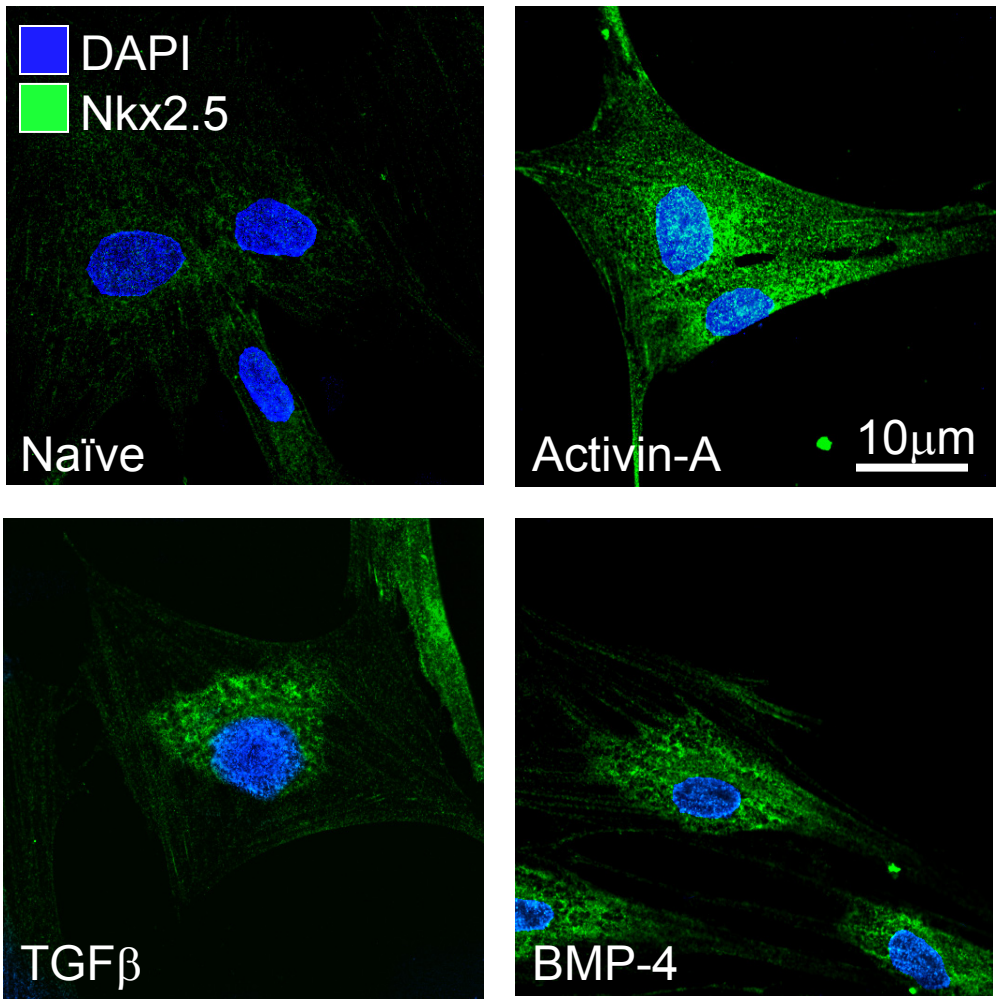

B

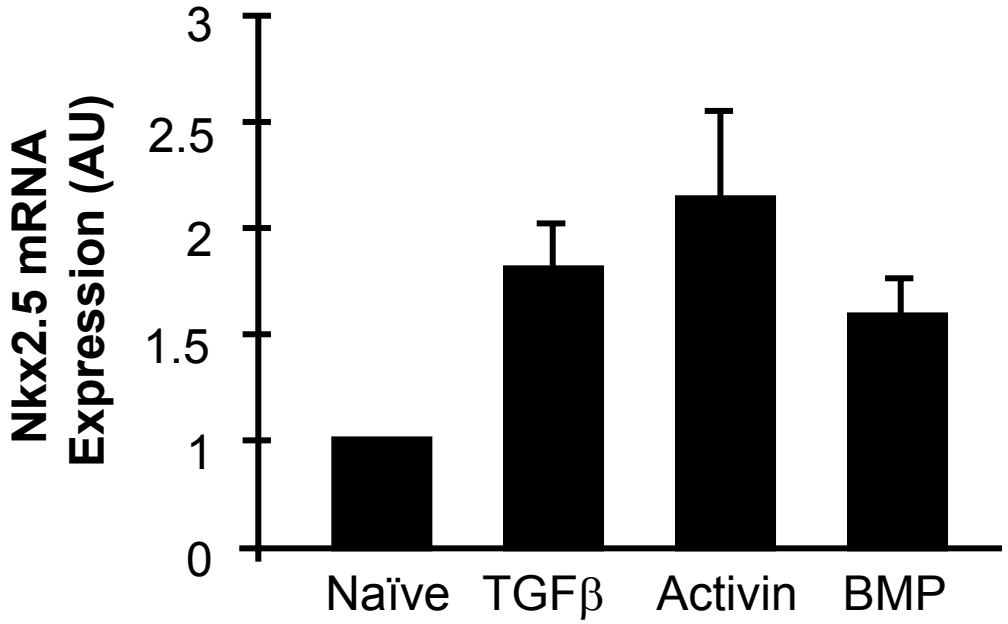

Supplemental Figure 2

A

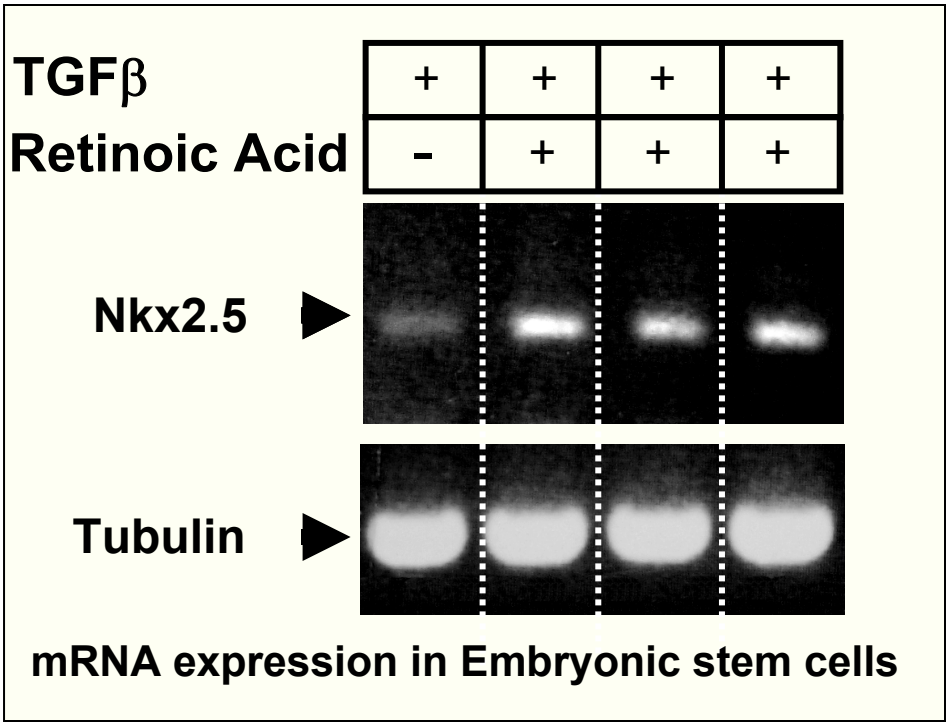

B

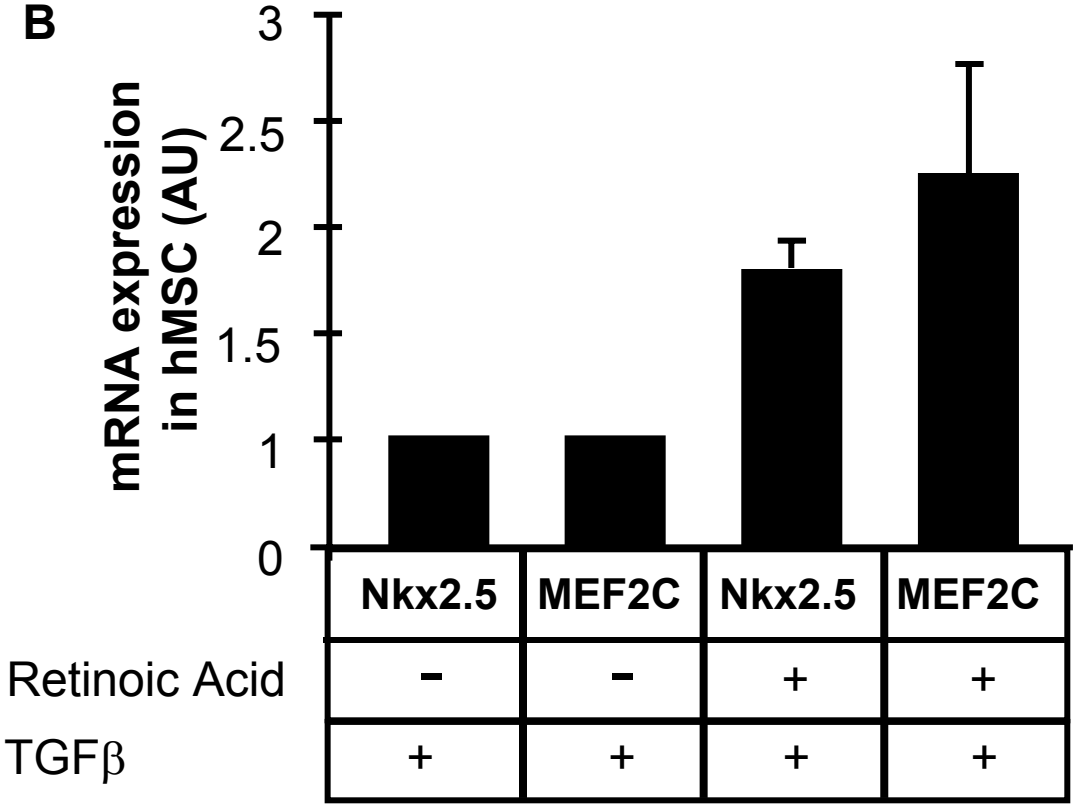

Supplemental Figure 3

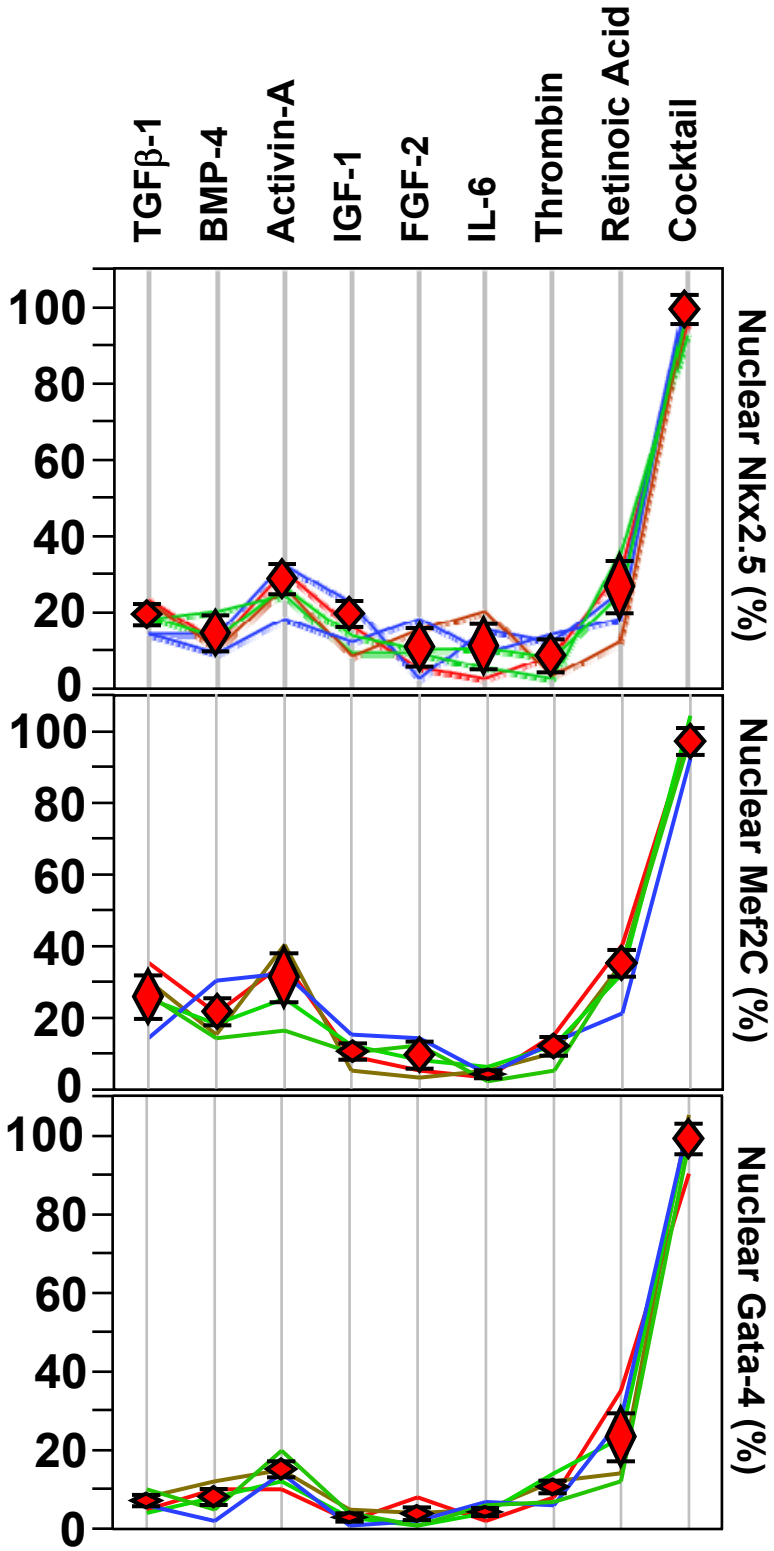

Supplemental Figure 4

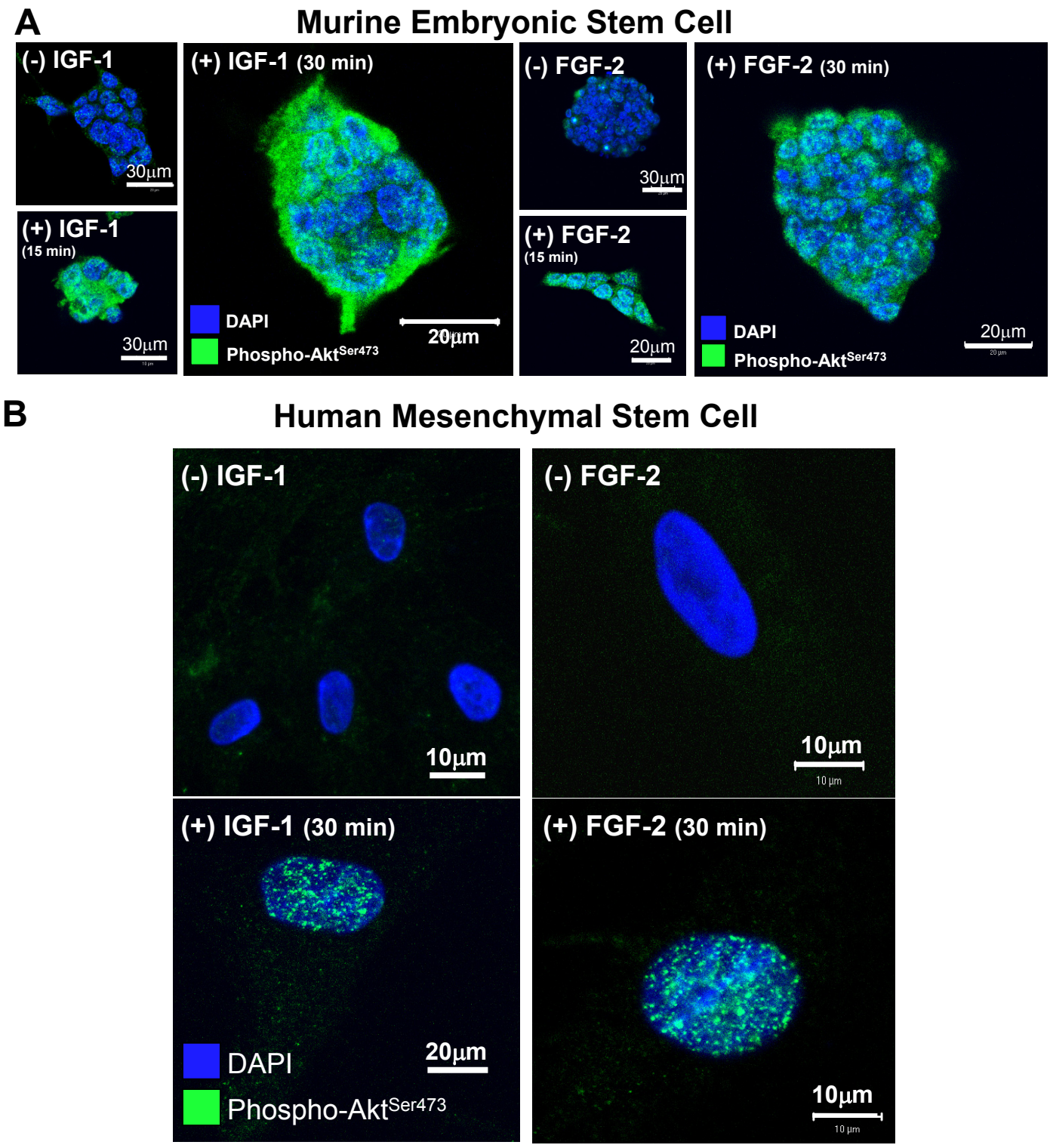

Supplemental Figure 5

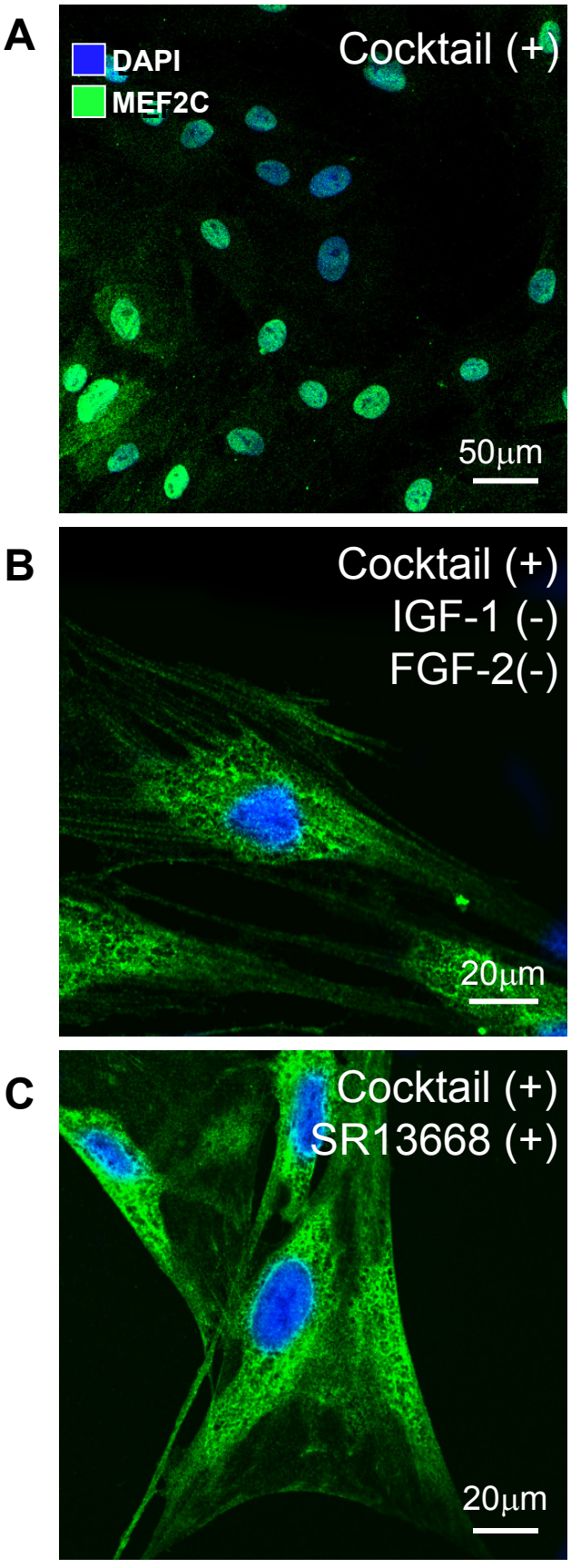

Supplemental Figure 6

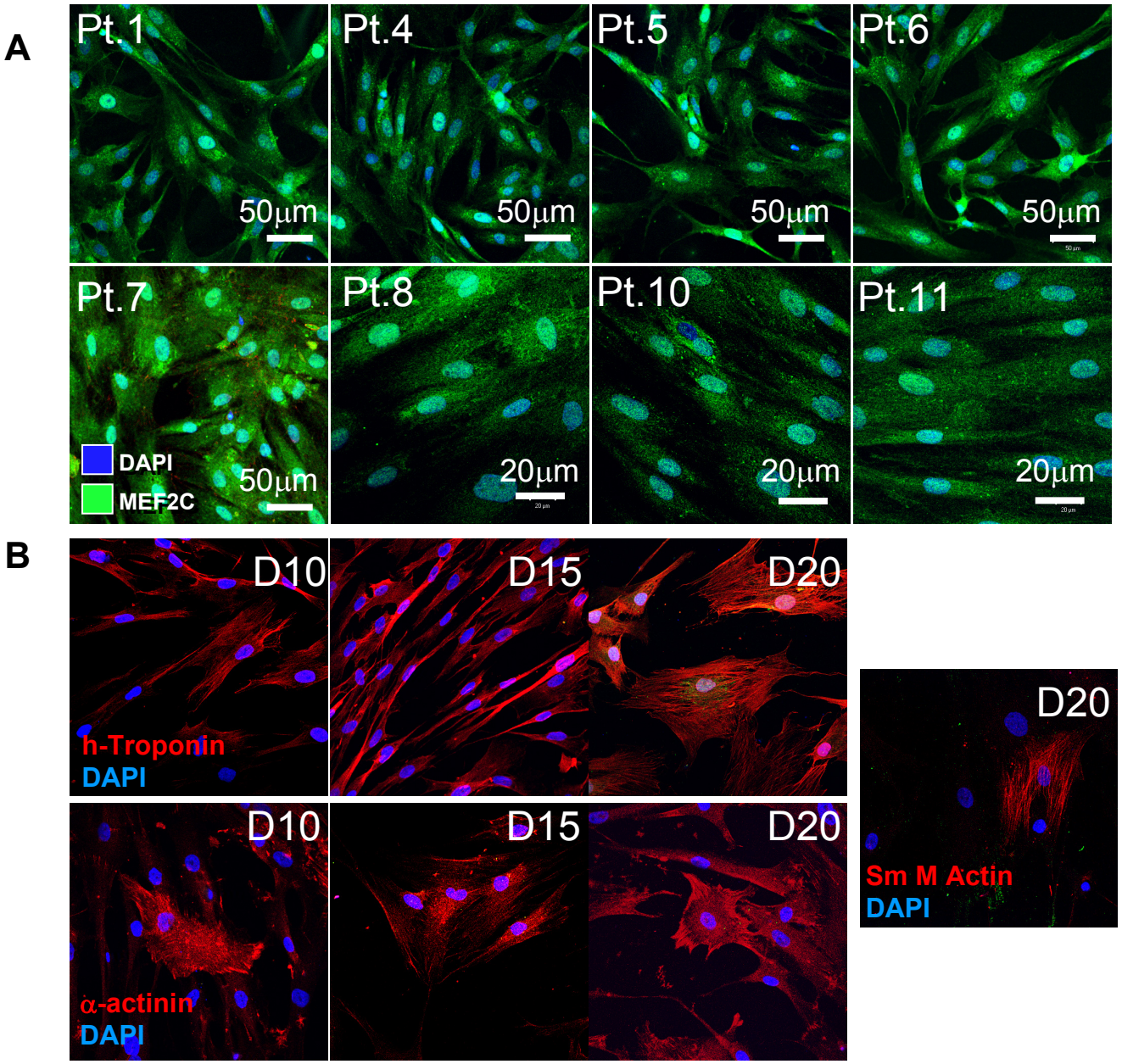

Supplemental Figure 7

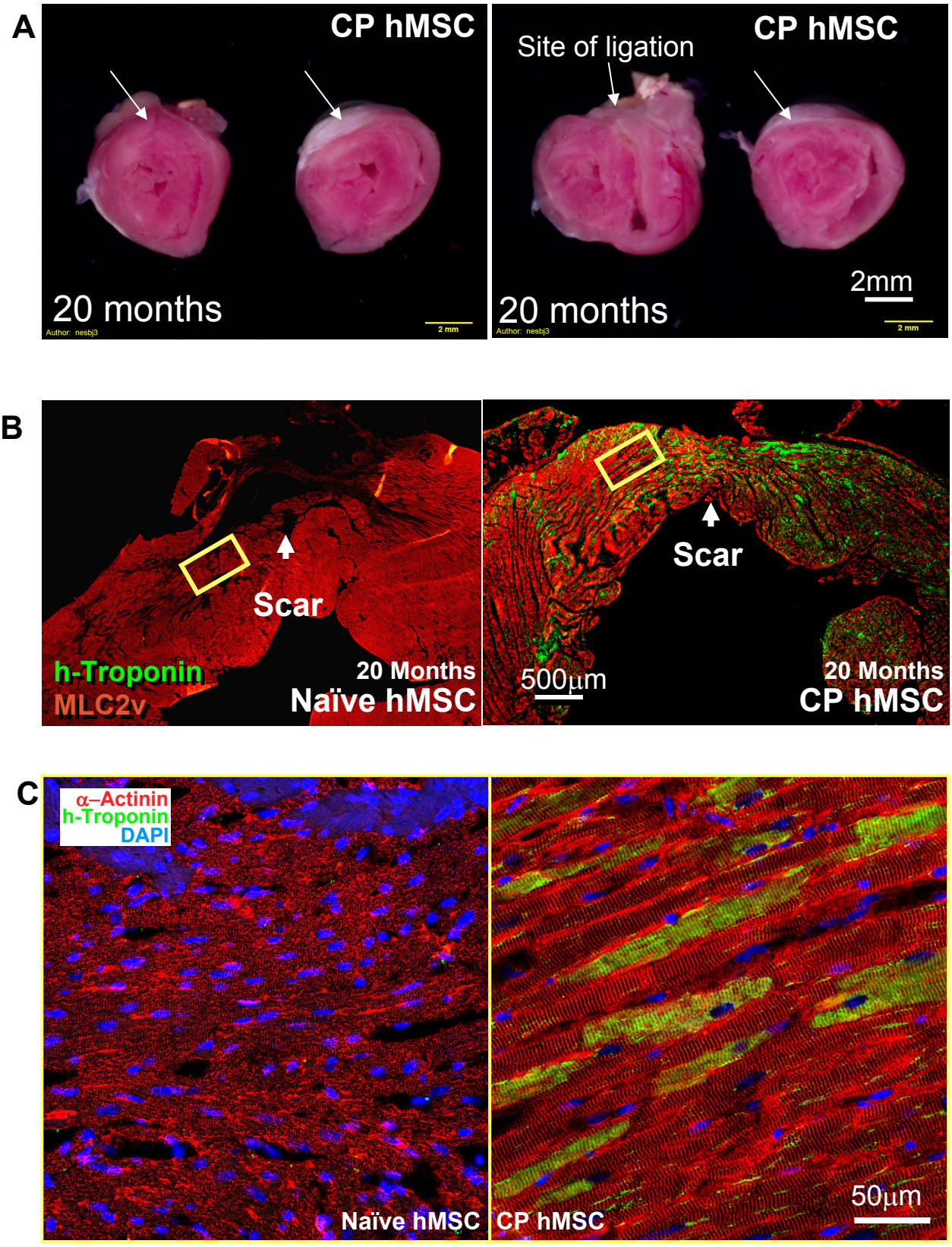

Supplemental Figure 8

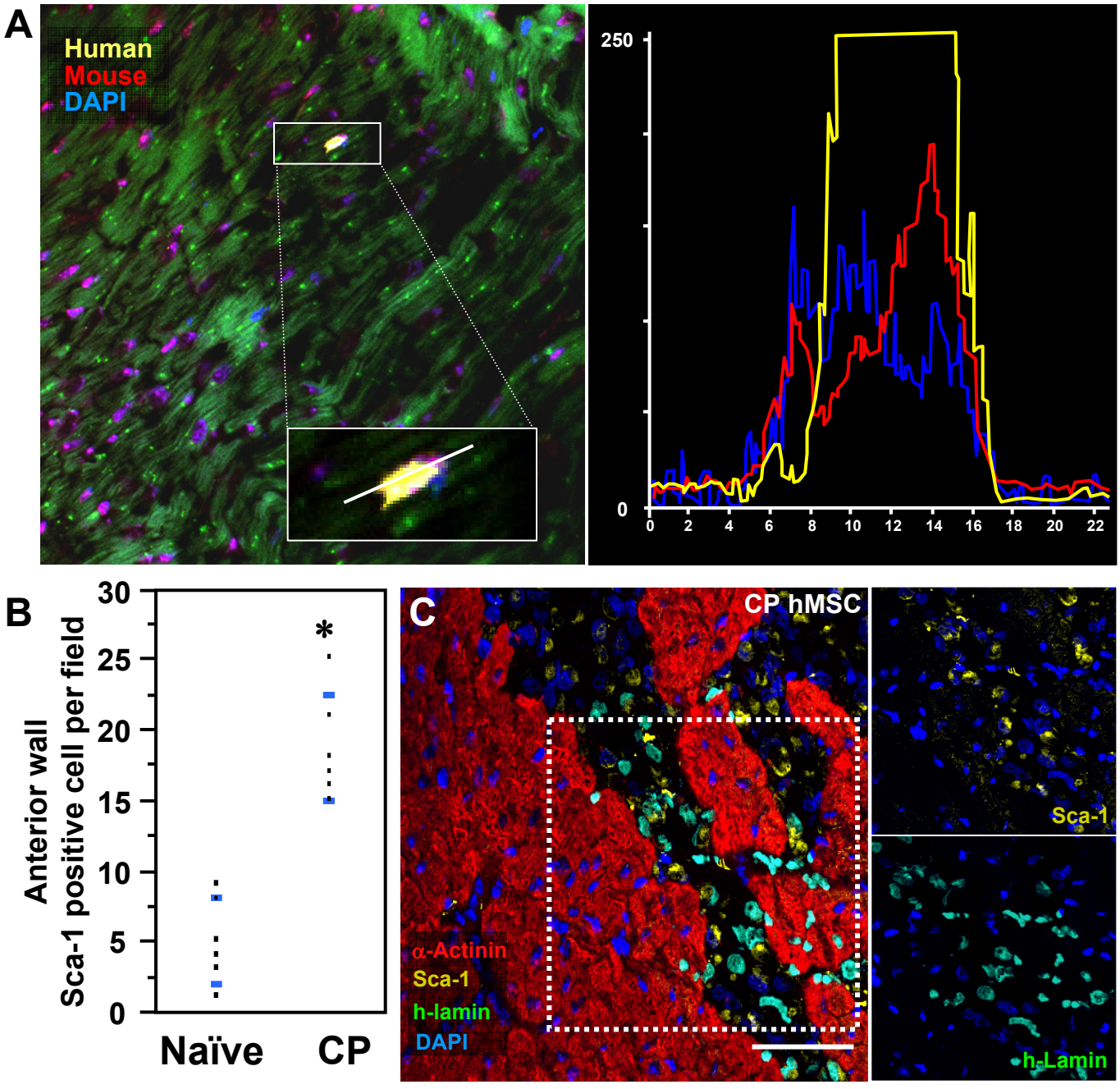

Supplemental Figure 9

hMSC Treated murine hearts demonstrate no tumor formation

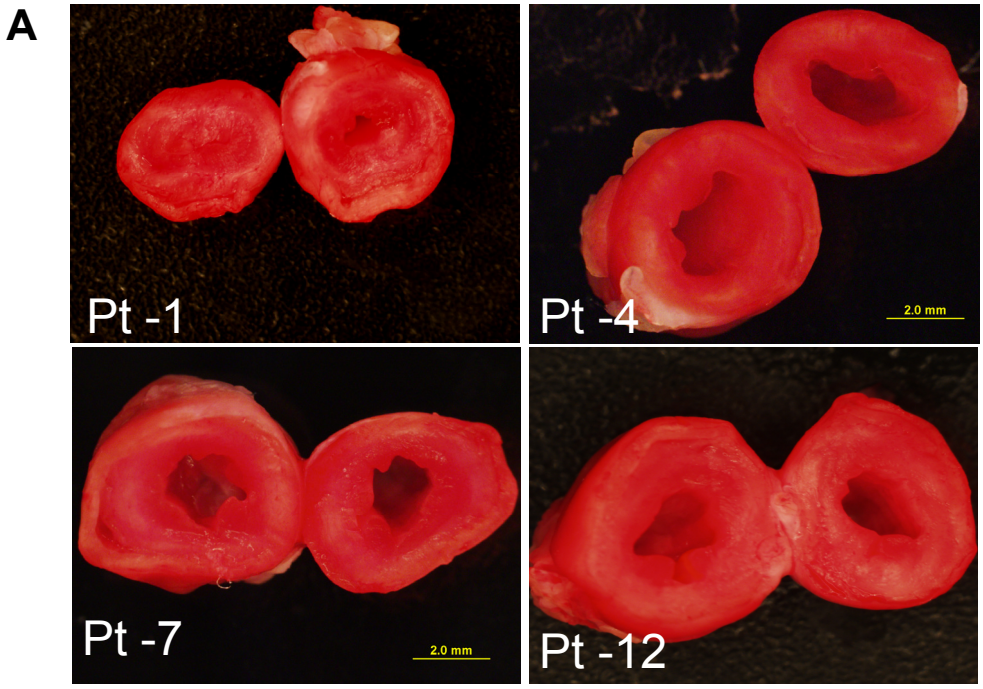

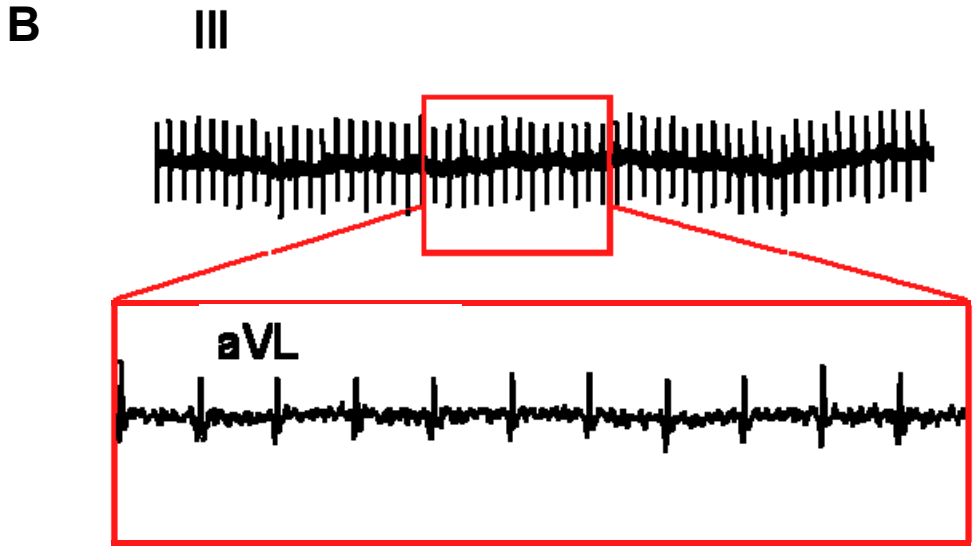

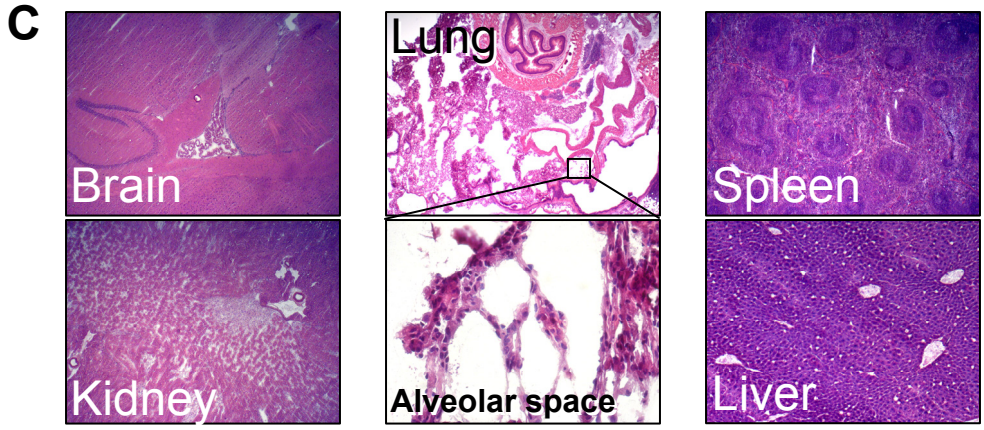

Supplemental Figure 10